Safety Analysis of the FASt TEst Reactor (FASTER) Preconceptual Design

Tyler Sumner, Anton Moisseytsev, James Sienicki, Florent Heidet

Argonne National Laboratory
9700 South Cass Avenue
Argonne, IL 60439

Abstract

The FASt TEst Reactor (FASTER) plant is a sodium-cooled fast spectrum test reactor design that was developed as part of an advanced demonstration and test reactor study, and provides high levels of fast and thermal neutron flux for scientific research and development. The 120 MWe FASTER plant has been designed with extended testing capabilities in mind, while keeping the design as simple as possible in order to make it efficient and cost attractive. The main function of the reactor is to provide neutrons for irradiation testing utilizing existing proven technologies to ensure a high technology readiness level. A preliminary safety analysis was performed of the FASTER design using the fast reactor safety analysis code SAS4A/SASSYS-1 to assess the reactor's safety performance during beyond design basis accidents. Three types of transient scenarios were analyzed for the FASTER design: unprotected transient overpower, unprotected loss of heat sink, and unprotected station blackout. These transients were simulated at beginning of equilibrium cycle and end of equilibrium cycle conditions. For each transient, failures of both the primary and secondary reactor scram systems were assumed. Because of the favorable reactivity feedbacks, relatively low peak fuel, cladding, and coolant temperatures were obtained during the transients and the reactor vessel temperature remained well below the limit for ensuring structural stability.

Keywords: FASTER, Sodium-Cooled Fast Reactor, SAS4A/SASSYS-1, Safety.

1. Introduction

Under a Department of Energy Advanced Demonstration and Test Reactor (ADTR) planning study, point designs of a select number of reactor design concepts were commissioned to provide a deeper technical basis for evaluation. (D. Petti , INL) The FASt TEst Reactor (FASTER) plant is a sodium-cooled fast spectrum test reactor design that was developed during this study. FASTER provides high levels of fast and thermal neutron flux to support development and qualification of fuels, materials, and other important reactor components of both thermal and fast neutron-based Generation-IV (Gen-IV) advanced reactor systems.

FASTER has been designed with extended testing capabilities in mind, while keeping the reactor as simple as possible to make it efficient and cost attractive. The main function of the reactor is to provide neutrons for irradiation testing utilizing existing proven technologies to ensure a high technology readiness level. The FASTER reactor plant relies upon the liquid metal base technology developed in the U.S. for EBR-II, FFTF, CRBR, and the ALMR program with a special emphasis on the irradiation testing capabilities developed for EBR-II and FFTF.

The safety goals in nuclear power reactor design and operation are to ensure the health and safety of the public, to protect the plant operating staff from harm, and to prevent plant damage. Traditionally, these goals have been fulfilled by an approach that 1) minimizes risk by maximizing safety margins in design and operation, 2) reduces the likelihood of potentially harmful events by providing safety systems to deal with anticipated events, and 3) provides additional design features to mitigate the harmful consequences of low probability events. The FASTER safety design approach implements this "defense in depth" strategy by adopting the traditional three levels of safety.

To ensure the first level of safety, design features have been selected that provide significant safety margin through inherent safety responses to upset conditions and equipment failures. The selection of liquid sodium coolant and metallic fuel with a pool-type primary system arrangement provides a highly reliable reactor system with large safety margins between normal operating conditions and limiting failure conditions. The coolant thermophysical properties provide superior heat removal and transport characteristics at low operating pressure with a large temperature margin to boiling. The metallic fuel operates at a relatively low temperature, below the coolant boiling point, due to its high thermal conductivity. The pool-type primary system confines all significantly radioactive materials within a single vessel, allowing for easy removal and replacement of components as well as shutdown heat removal by natural circulation.

The normal process of performing safety assessments considers a spectrum of design basis accidents (DBAs) as tests of the various safety systems. These DBAs generally assume single failures. Accidents within the design basis must be accom-

Email address: tsumner@anl.gov (Tyler Sumner)

modated by the design and shown to limit risks to the public that are within regulatory standards. Beyond the design basis, there exists a class of accidents of such low probability that they have been termed hypothetical. These beyond design basis accidents (BDBAs) involve multiple concurrent failures of safety grade systems, and usually are considered to have a frequency of less than 10^{-6} per reactor-year. Because of the potentially severe consequences of accidents in this class, they have received significant regulatory scrutiny in prior sodium-cooled fast reactor licensing reviews for the purpose of characterizing thermal and structural safety margins beyond the design basis.

The proposed FASTER design is capable of accommodating various beyond design basis accidents without producing high temperatures and conditions that might lead to a severe accident, such as coolant boiling, cladding failures, or fuel melting. The inherent neutronic, hydraulic, and thermal performance characteristics of the FASTER design provide self-protection during these accidents to limit accident consequences without activation of engineered systems or operator actions.

For the FASTER preliminary safety analysis, three accident scenarios, during which both reactor scram systems fail to insert the control and safety rods, were simulated to assess the reactor's safety performance during BDBA transients and demonstrate the reactor's inherent and passive safety capabilities. In the unprotected transient overpower (UTOP) sequence, one control rod withdraws. In the unprotected loss-of-heat-sink (ULOHS) accident, heat removal through the power conversion system is lost. In the unprotected station blackout (USBO) sequence, power is lost to all primary and secondary coolant pumps. Taken collectively, these three accident initiators encompass the three primary ways that an operating reactor can be perturbed, i.e. by a change in reactivity, by a change in coolant inlet temperature, or by a change in coolant flow.

This paper presents the FASTER preliminary safety analysis, and is supplemented by two companion papers. The first companion paper provides an overview of FASTER, the ADTR study, and the design philosophy and objectives that were targeted. (F. Heidet, 2018a) The second companion paper provides an in depth view of the FASTER core design and the neutronics performance it achieves. (F. Heidet, 2018b)

2. SAS4A/SASSYS-1 Model

The SAS4A/SASSYS-1 (Fanning, 2017) code was used to analyze the safety performance of the FASTER reactor design. SAS4A/SASSYS-1 is a sodium fast reactor safety analysis tool developed by Argonne National Laboratory beginning in the 1960s with an extensive validation history. Recent validation efforts have focused on comparisons against whole plant measured data from several EBR-II shutdown heat removal tests, analyzed as part of an IAEA coordinated research project, FFTF loss of flow without scram tests, which will be the subject of an upcoming IAEA CRP. (INTERNATIONAL ATOMIC ENERGY AGENCY, 2017)

Because the FASTER concept is still in the preliminary design phase, some aspects of the design are further developed than others. Models of the core and primary heat transport system (PHTS) were created based on the current design. The intermediate heat transport system (IHTS) and direct reactor auxiliary cooling system (DRACS) designs are less developed so models of those systems were created by modifying the IHTS and DRACS models from similar pool-type SFR designs. The SAS4A/SASSYS-1 model used for the FASTER safety analysis is described in the sections below.

2.1. Core Model

In SAS4A/SASSYS-1, the thermal-hydraulic performance of a reactor core is analyzed with a model consisting of a number of single-pin channels. Each single-pin channel represents the fuel, cladding, coolant, and structure of an average pin in an assembly and assemblies with similar reactor physics and thermal-hydraulic characteristics are grouped together. One or more single-pin channels can be used to represent all the fuel pins in a reactor core. SAS4A/SASSYS-1 models include axial zones to represent the fueled and gas plenum regions as well as up to six upper and lower reflector zones. Each axial zone is also connected to a structure region, which can be used to model components such as the wire-wrap or duct walls. At each axial location, temperatures are calculated at multiple radial nodes in the fuel, cladding, reflectors, and structure. A single bulk coolant temperature is assumed at each axial location. One-dimensional, radial heat transport calculations are performed at each axial segment from the fuel, through the cladding and into the coolant. Heat transfer is also calculated from the coolant to the gas plenum, reflector, and structure regions. The momentum equation is solved to determine the axial coolant flow. Convective heat transfer is assumed to dominate so axial heat conduction is neglected.

For the preliminary FASTER safety analysis, each SAS4A/SASSYS-1 channel represents all assemblies of one type (fuel, reflector, test, shield, control, and graphite). The one exception is for the fuel assemblies, where the assemblies in the inner and outer regions of the core were represented by two channels, which have identical geometries. The differences between the inner and outer core fuel channels are related to the plutonium content arising from different burn-up rates in the different regions of the core, which affects fuel properties such as thermal conductivity, the assembly-wise power production and flow rate, and the reactivity feedback coefficients. In addition to these "regular" channels, a peak channel was included to calculate peak temperatures during the transients. Table 1 lists the seven regular channels and one peak channel along with the power and flow per assembly for each channel and Figure 1 presents the core channel map. Steady-state assembly power and flow values were calculated with PERSENT and SuperEnergy-2, respectively. (Smith, 2013; K. L. Basehore and N. E. Todreas, 1980) Assembly outlet temperatures, given for both beginning-of-equilibrium-cycle (BOEC) and end-of-equilibrium-cycle (EOEC) conditions, represent assembly power-to-flow ratios. Flow orifice zones are assumed to be fixed during the fuel cycle so the steady-state assembly flow distribution is the same for BOEC and EOEC conditions for the regular channels.

Table 1: Core Model Channels

	Type	Pins Per Assembly	Assemblies	Power Per Assembly BOEC/EOEC (MW)	Flow per Assembly (kg/s)	Outlet Temp. BOEC/EOEC (°C)
1	Inner Core	271	30	6.30/6.25	31.6	512.4/511.3
2	Outer Core	271	25	4.15/4.19	21.4	507.3/509.0
3	Control	91	9	0.078/0.080	0.359	504.1/505.3
4	Test	91	39	0.065/0.068	0.327	506.8/510.5
5	Reflector	91	77	0.047/0.048	0.231	502.9/507.4
6	Graphite	91	22	0.0006/0.0007	0.004	472.5/476.2
7	Shield	61	111	0.005/0.005	0.031	480.8/485.1
8	Peak Core	1	1	7.61/3.70[1]	30.9/14.9[1]	548.9/550.0

[1] Equivalent 271-pin assembly values

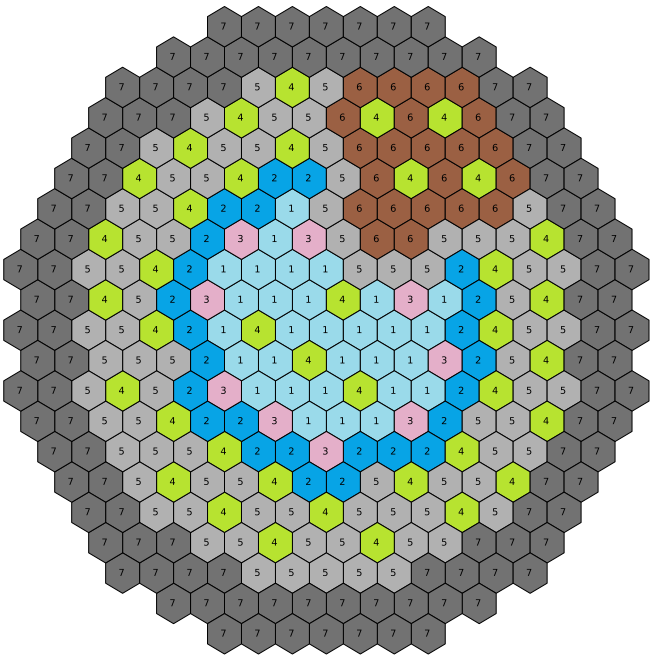

Figure 1: SAS4A/SASSYS-1 Core Channels

The peak channel in the model, which is represented by a single pin, was introduced to calculate maximum temperatures in the core. Power production in the peak channel is the average per-pin power of the assembly where this peak coolant temperature was calculated. The peak channel flow rate was reduced from the average assembly flow rate so that the coolant outlet temperature for the peak pin matches the maximum coolant outlet temperature calculated in the SuperEnergy-2 calculations to account for sub-channel flow variations within the assemblies. The assemblies corresponding to the peak coolant temperature locations are different for BOEC and EOEC conditions. Therefore, both the power and flow rate for the peak pin are different for the BOEC and EOEC models.

Figure 2 illustrates the axial geometry of the different channel types in the core model. Most of the core model dimensions are available in the FASTER neutronics companion paper. (F. Heidet, 2018b) Zones 1 and 2 represent the lower reflector in the fuel channels. Zone 1 is a 0.85 m long block-type reflector with three semi-circular coolant channels. Zone 2 is a 10 cm long transition zone from the block-type reflector to the fuel pins. It is modeled as solid structure with a central coolant channel. Zone 3 includes the fuel and fission gas plenum regions, which are 0.8 m and 0.52 m tall, respectively. These heights reflect the hot (i.e., at operating temperature) dimensions for irradiated fuel. There are 20 axial segments in the fuel zone and 5 axial segments in the fission gas plenum. Zones 4-6 represent the upper reflector. The first two zones are similar to the lower reflector zones, but inverted. Zone 4 is the transition from fuel pins to the block-type upper reflector and Zone 5 has the same geometry as the lower block-type reflector zone, Zone 1. The final upper reflector zone, Zone 6, is the fuel handling socket region.

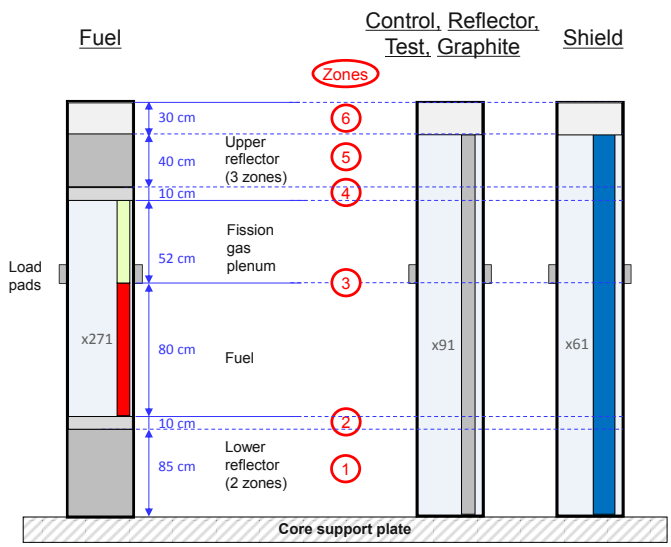

Figure 2: SAS4A/SASSYS-1 Core Channel Axial Geometry

The fuel channel geometry is identical for BOEC and EOEC conditions. In both cases, the fuel is conservatively assumed to have expanded into contact with the cladding inner surface, which increases the fuel centerline temperature by reducing the fuel thermal conductivity and displacing the very high thermal

conductivity sodium from the gap. The FASTER's fuel has an 85% smear density so the fuel expands into contact with the cladding at lower burn-ups than for more traditional metallic fueled designs with a 75% smear density. For BOEC conditions, assuming fuel-cladding contact corresponds to a minimum fuel burn-up of 1%, rather than fresh fuel. This is an acceptable assumption because only a fraction of the fuel will be fresh at the very beginning of the BOEC cycle.

As shown in Table 1, the test and graphite assemblies have very small contributions to the total core power and flow. Therefore, uncertainties in the geometry of these assemblies, which are still being developed for FASTER, will not significantly affect the results of safety analysis. For this analysis, the test assemblies were assumed to contain no fuel. In the future the transient scenarios discussed in this paper should be analyzed on the case-by-case basis to account for the specific compositions of the assemblies in the test positions. Because the graphite and test assemblies produce very little power and have very little flow, they are assumed to have exactly the same geometry as the reflector assemblies, i.e. 91 HT9 rods spanning the entire assembly height. Because a negative coolant void worth was calculated for these assemblies, modeling the test assemblies with steel rods rather than entirely sodium will lead to conservative safety margins. Replacing a portion of the coolant with structure in these assemblies results in a less negative coolant density reactivity feedback for transients where the coolant temperature increases.

The control assemblies are currently modeled as being at the fully insertion position, as illustrated in Figure 2. This approach preserves the geometry of the control assemblies, but does not account for the fact there will be more sodium in the core region when the control rods are withdrawn. To account for this difference, the coolant void reactivity input for the control channel was corrected by a multiplication factor to preserve the total coolant void worth in the SAS4A/SASSYS-1 steady-state calculations. It should be noted that the neutronics analysis was performed with the rods at the critical control rod position.

The FASTER core model calculates heat transfer between neighboring assemblies. Heat transfer coefficients were calculated to account for the thermal resistance of the nominal 3 mm inter-assembly sodium gap, which is assumed to be filled with stagnant sodium, and two halves of the outer duct wall node thickness, one on each side of the gap. Channel-to-channel heat transfer mostly affects the temperatures in the non-fueled assemblies, which do not represent any limiting conditions in the unprotected transients. In the fueled regions of the core, the assembly-to-assembly heat transfer rate is small compared to the power generation with the channel-to-channel heat transfer model only affecting steady-state temperatures by 1°C.

2.2. *Primary and Intermediate Heat Removal Systems Model*

The PRIMAR-4 module simulates the thermal hydraulics of the primary, intermediate, and direct reactor auxiliary cooling systems in SAS4A/SASSYS-1. Compressible volumes (CV) are zero-dimensional volumes that are used to represent larger volumes of coolant, typically inlet and outlet plena or pools, as well as pipe tees. CVs, which are characterized by their pressure, temperature, elevation, and volume, are connected by liquid segments, which are composed of one or more elements. Elements are modeled by one-dimensional, incompressible, single-phase flow and can be used to model pipes, valves, pumps, heat exchangers, steam generators, and more. Elements are characterized by their pressure, temperature, elevation, and mass flow rate.

Figure 3 illustrates the PRIMAR-4 model of the primary heat transport system (PHTS). As the intermediate system and DRACS designs are still being developed, those models are not illustrated here. It should be noted that because the models of those systems were calibrated to obtain their ultimate system performances, changes to the pipe lengths or diameters will not significantly affect the results.

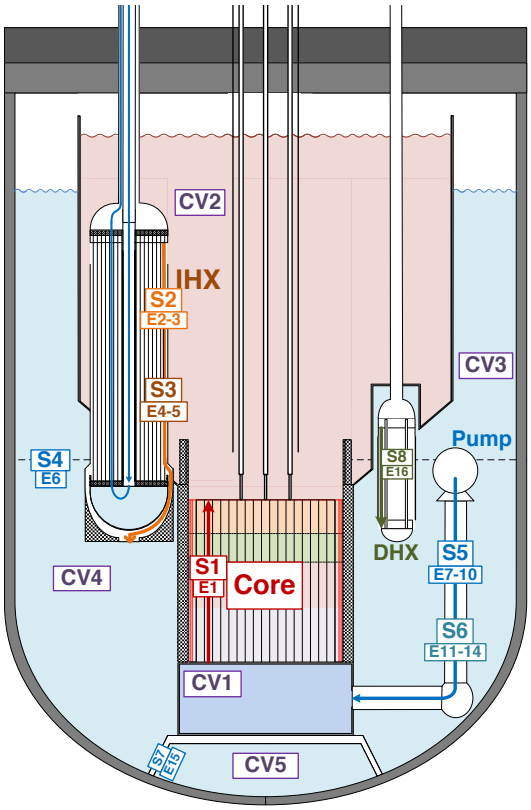

Figure 3: SAS4A/SASSYS-1 Model of the Primary Sodium Heat Transport System

Element 1 represents the eight core channels. At steady-state, sodium enters the core from the inlet plenum (CV1) at a temperature of 355°C and discharges into the hot pool (CV2) at an average of 510°C. Element 2 represents the primary-side, i.e. shell-side, of IHXs 1 and 2 and Element 4 represents the primary side of IHXs 3 and 4.

Because the heat exchangers are identical, the multiplicity feature in SAS4A/SASSYS-1 is used to represent the first two heat exchangers with one element and the other two heat exchangers with another element. SAS4A/SASSYS-1 has a limit of 4 heat exchangers so the decay heat exchangers (DHX) could not be modeled if all four IHXs were modeled separately. Elements 3 and 5 represent the IHX outlets with sodium discharged

into CV4, the bulk portion of the cold pool. The primary-side outlet of the IHXs is located one meter above the top of the active fuel to promote natural circulation during loss of forced circulation conditions.

CV3 represents the upper portion of the cold pool and feeds the two DHXs. In pool-type SFRs, thermal stratification and heat transfer between the hot and cold pools through the redan produce higher temperatures in the upper portion of the cold pool. The component-to-component heat transfer model was used to specify heat transfer between the upper cold pool and the hot pool, which produces higher temperatures in CV3 than in CV4.

CV5 represents a very small portion of sodium at the bottom of the cold pool. This volume does not play a significant in the transients analyzed but was reserved for modeling the stagnant sodium at the bottom of the cold pool. Additional analysis is required to determine exactly how much sodium stagnates after the primary sodium pumps trip.

In the intermediate heat transport systems, a simple steam generator model provides the boundary for both intermediate loops.

Element 16 represents the shell-side of the decay heat exchangers for the direct reactor auxiliary cooling system. As with the IHXs, multiplicity is used to model two heat exchangers with one element. The third DHX is not modeled because one of the DRACS units is assumed to be unavailable for these analyses.

Segment 17 represents the intermediate side of the direct reactor auxiliary cooling system. Since sodium in the DRACS operates under natural circulation conditions, there is no pump. The air mass flow rate through the air dump heat exchanger (AHX) is also governed by natural circulation based user-input loss coefficients and air-side temperatures. When fully operational at nominal reactor temperatures, a single AHX rejects 0.25% of the nominal core power level (0.75 MW) for a total of 0.75%. However, for these safety analyses, one of the three units was assumed to be offline and unavailable due to maintenance, leaving a total heat rejection rate of 0.5%.

2.3. Reactivity Feedbacks

The SAS4A/SASSYS-1 model calculates the following reactivity feedbacks:

- Fuel Doppler,
- Fuel density (and axial expansion),
- Cladding (structure) density,
- Coolant voiding,
- Control rod movement, including control rod driveline, reactor vessel, and below-the-core structures expansion, and
- Core radial expansion.

The Doppler, axial expansion, cladding density, and coolant void reactivity feedback coefficients that are used in the SAS4A/SASSYS-1 model were generated using first order perturbation theory with the PERSENT code (version 11.0) utilizing P5 transport calculations from DIF3D-VARIANT. (Smith, 2014) PERSENT calculated effective delayed neutron fractions of 3.32E-03 at BOEC and 3.33E-03 at EOEC conditions. The radial expansion and control rod expansion feedbacks were calculated based on eigenvalue differences. The first three feedbacks are applicable to the fueled assemblies only (Channels 1 and 2).

Table 2 lists the total reactivity worths for the feedback effects for each channel at BOEC and EOEC conditions. Note that these results are the total worths for each channel, not per assembly. The cladding and fuel worths were calculated only for the fueled channels, Channels 1 and 2. Channel 3 has the largest void worth due to the large coolant volume fraction, especially at EOEC conditions when the control rods are withdrawn. Most of the individual and total reactivity coefficients are similar for BOEC and EOEC conditions. The only noticeable exception is the void worth for the control channel, where some portion of the coolant is displaced from the core zone by partially inserted control rods at BOEC conditions.

The core radial expansion feedback in the transient simulations was calculated using the simple radial expansion model. This model, which is represented by Equation 1, neglects assembly bowing and assumes straight-line expansion between the core support plate and above-core load pads to determine the average expansion of the core at the core midplane, as illustrated in Figure 4. XAC represents the distance from the grid plate to the above core load pads and XMC represents the distance from the grid plate to the core midplane. For FASTER, the XMC/XAC ratio is 0.771. The coefficient C_{re} was calculated based on the core reactivity change for an assumed 1% increase in the assembly pitch with a corresponding decrease in atom density of the structures and fuel to preserve mass. The 1% change in pitch is then converted to a change in temperature based on the thermal expansion coefficient for the selected structural material.

$$\rho_{re} = C_{re}\left[\Delta T_{in} + \frac{XMC}{XAC}\left(\Delta T_{SLP} - \Delta T_{in}\right)\right] \tag{1}$$

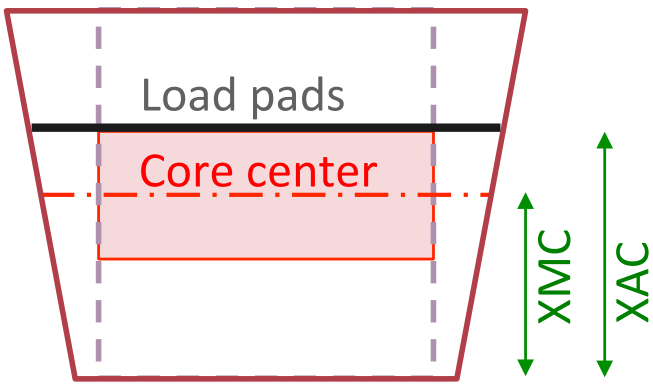

Figure 4: SAS4A/SASSYS-1 Simple Radial Expansion Model

Because the simple radial expansion model supports only a single input for C_{re}, the value of C_{re} that was input for each transient depends on the expected dominant component. For station blackout and transient overpower accidents, core radial expansion is dominated by the temperature rise in the core and,

Table 2: Reactivity Feedback Coefficients by Channel

BOEC Conditions						
Channel	Type	Void ($)	Clad ($)	Fuel ($)	Unvoided Doppler ($T\Delta K/\Delta T$)	Voided Doppler ($T\Delta K/\Delta T$)
1	Inner Core	-0.67	-3.51	116.2	-0.0020	-0.0016
2	Outer Core	-1.17	1.27	40.6	-0.0010	-0.0009
3	Control	-2.17	0	0	0	0
4	Test	-0.41	0	0	0	0
5	Reflector	-0.59	0	0	0	0
6	Graphite	-8×10^{-7}	0	0	0	0
7	Shield	-0.02	0	0	0	0
Reactor Total		**-5.03**	**-2.24**	**156.8**	**-0.0031**	**-0.0025**
EOEC Conditions						
Channel	Type	Void ($)	Clad ($)	Fuel ($)	Unvoided Doppler ($T\Delta K/\Delta T$)	Voided Doppler ($T\Delta K/\Delta T$)
1	Inner Core	-0.51	-4.04	110.2	-0.0022	-0.0017
2	Outer Core	-1.35	1.38	42.8	-0.0012	-0.0010
3	Control	-2.66	0	0	0	0
4	Test	-0.43	0	0	0	0
5	Reflector	-0.66	0	0	0	0
6	Graphite	-7×10^{-7}	0	0	0	0
7	Shield	-0.02	0	0	0	0
Reactor Total		**-5.62**	**-2.66**	**153.0**	**-0.0034**	**-0.0027**

Table 3: Core Radial Expansion Reactivity Feedback Coefficients

C_{re} ($\$/K$)	BOEC	EOEC
USBO and UTOP	-3.150×10^{-3}	-3.193×10^{-3}
ULOHS	-4.383×10^{-3}	-4.441×10^{-3}

therefore, the expansion of the load pads. The thermal expansion coefficient for the load pad material, HT9, evaluated at the steady-state core-outlet temperature ($1.379\cdot10^{-5}1/K$) was selected and used to determine the C_{re} coefficient. For loss of heat sink transients, the core-inlet temperature changes faster than the core outlet temperature so the core radial expansion feedback is dominated by the expansion of the core support plate. Therefore, the material properties of the Type 316 stainless steel support plate, evaluated at the steady-state core inlet temperature, were used for the thermal expansion coefficient ($1.919\cdot10^{-5}K^{-1}$) and the C_{re} input. Additionally, for the ULOHS transient it was conservatively assumed that the above-core load pads remain in contact even when the core support plate expands. The values of the C_{re} coefficient for each transient are presented in Table 3.

The control rod driveline (CRDL) expansion feedback is calculated in SAS4A/SASSYS-1 based on a second-order approximation of the control rod position relative to the critical position:

$$\rho_{CR} = A_{CRDEX}\Delta z + B_{CRDEX}\Delta z^2 \quad (2)$$

where Δz is the relative change in the control rod position in the core as a function of time. Vessel expansion, which causes the bottom-supported core to be pulled away from the control rods, was calculated using the control system module. The coefficients ACRDEX and BCRDEX were obtained using a quadratic fit of the control rod worth curve (S-curve). To account for the movement of all control rods, the total reactivity feedback was calculated as the sum of the feedback from both the primary and secondary control rods. These values are given in Table 4 for both BOEC and EOEC conditions.

For the UTOP transient, the single most reactive control rod is assumed to have withdrawn from the core, so the ACRDEX and BCRDEX coefficients for primary control rods are calculated based on the "All-minus-one" control rod worth curve, which accounts for movement of all control rods except for the rod already withdrawing from the core, which initiated the transient. No calculations were done for the UTOP transient at EOEC conditions because the control rods will be almost fully withdrawn from the core, resulting in a benign transient progression. Because the control rods are partially inserted at BOEC conditions, the CRDL feedback is much stronger than at EOEC conditions. The CRDL effect represents the most significant difference between the BOEC and EOEC results for the unprotected transient simulations presented below since the rest of the reactivity feedbacks are similar for BOEC and EOEC conditions.

The control rod insertion depth in the core is affected by expansions of the control rod drivelines, reactor vessel, and

Table 4: CRDL Expansion Reactivity Feedback Coefficients

Transient	Coefficient	BOEC	EOEC
USBO and ULOHS	ACRDEX($\$/m$)	-36.68	-10.96
	BCRDEX($\$/m^2$)	-48.85	-68.89
UTOP	ACRDEX($\$/m$)	-30.47	N/A
	BCRDEX($\$/m^2$)	-42.66	

Table 5: Transient Initiators

Initiator	UTOP	ULOHS	USBO
PHTS Pumps Trip			✗
IHTS Pumps Trip		✗	✗
Feedwater Pumps Trip		✗	✗
Single Control Rod Withdrawal	✗		

core support structures. The control rod and control rod drivelines were expanded together as one component with a nominal length of 9.92 m. For transients where the cold pool temperature rises, reactor vessel expansion lowers the core away from the control rods, which effectively withdraws the control rods. For the ULOHS and USBO transients, this effect provides the most significant positive reactivity feedback. As the drivelines expand, the control rods are inserted further into the core. It was assumed that below the bottom of the active fuel, reactor vessel expansion and core support structure expansion occur at the same rate and magnitude and they therefore cancel each other out. The total length of the reactor vessel that was considered to expand was 8.08 m, which is the length from the cold pool sodium level to the bottom of the active fuel.

3. Results

Three types of transients were simulated with the SAS4A/SASSYS-1 fast reactor safety analysis code:

- Unprotected transient overpower (UTOP),
- Unprotected loss of heat sink (ULOHS), and
- Unprotected station blackout (USBO).

In each scenario, it was assumed that the Reactor Protection System (RPS) fails to scram the control rods. Best estimate simulations were performed to determine the maximum temperatures that occur during each transient and ensure that acceptable margins to various safety limits are maintained. The transient initiators are summarized in Table 5 and each transient is fully defined in the sections below. Safety margins are also defined below.

A primary pump trip is initiated by quickly decreasing the pump torque to zero. The sodium flow rate coasts down according to the inertia of the pumps and, following the flow coast down, natural circulation flow is established. An intermediate pump trip is simulated in the same way as a primary pump trip.

Because the steam generators represent the boundary conditions in the SAS4A/SASSYS-1 model, the feedwater pumps were not modeled. To model the loss of heat rejection through the steam generators, which accompanies a feedwater pump trip, the temperature drop across the steam generators was quickly reduced to zero at the beginning of the ULOHS and USBO transients. For the UTOP scenario, the steam generator was conservatively assumed to maintain the steady-state heat rejection rate throughout the transient. In reality, increased sodium temperatures in the IHTS would produce higher steam generator heat rejection rates so this assumption leads to higher temperatures.

Each transient scenario was simulated at beginning-of-equilibrium-cycle (BOEC) conditions. The ULOHS and USBO transients were also simulated at end-of-equilibrium-cycle (EOEC) conditions. Because the primary and secondary control rods are already withdrawn at EOEC conditions, the UTOP transient initiator does not apply at EOEC.

The FASTER has three direct reactor auxiliary cooling system (DRACS) units, each providing a nominal heat rejection rate of 0.25% of the initial total reactor power level when fully activated. During the transient simulations, the DRACS air dampers are assumed to activate five seconds after the transient begins, representing a short delay between flow rate, temperature, or power measurements exceeding allowable limits and the reactor protection system providing the signal to activate the DRACS units. DRACS activation is assumed to occur over a five-second period. Before the DRACS units are activated and the air dampers open, the steady-state DRACS heat rejection rate predicted by SAS4A/SASSYS-1 is 0.09% per DRACS unit. Because the DRACS units are assumed to activate promptly after the start of each transient, the steady-state DRACS heat rejection rate does not significantly affect the transient results. All nominal heat rejection rates correspond to a Decay Heat Exchanger (DHX) primary-side sodium inlet temperature of 355°C.

For each transient, it was assumed that the air dampers in one of the DRACS units fail to open. To be conservative, it was assumed that zero heat rejection was available through that DRACS unit. In reality, a DRACS unit would provide a small amount of heat rejection, even if the air damper were completely closed. With only two DRACS units available, the nominal heat rejection rate is 0.5% for each transient. The heat rejection rate increases during the transient scenarios as the cold pool temperature increases.

3.1. Safety Margins

Maintaining coolable geometry within the core is the primary consideration when evaluating events with such low frequencies. For example, fuel melting can be tolerated at the center of the fuel pin as long as molten fuel is not breaching the cladding and entering the coolant channel. However, the favorable features of FASTER, and metallic-fueled SFRs in general (i.e., strong inherent reactivity feedbacks, the excellent heat

transfer capabilities of sodium, and the large heat sink of multiple sodium regions inside of the pool-type reactor vessel) lead to such large safety margins that the transient scenarios can be evaluated under higher scrutiny. For this analysis, the results of a transient are considered acceptable when reasonably large margins to sodium boiling and fuel melting are maintained.

For each transient scenario, the following safety margins were considered:

- Coolant boiling,
- Fuel melting,
- Cladding integrity, and
- Reactor vessel integrity.

SAS4A/SASSYS-1 automatically calculates the peak in-core fuel, cladding, and coolant temperatures, and these temperatures are reported for each transient in the sections below along with the coolant saturation temperature at the location of the peak coolant temperature. SAS4A/SASSYS-1 also reports the minimum margin to sodium boiling, which, because the sodium saturation temperature depends on pressure, may occur at a different location than the peak sodium temperature.

The FASTER model uses fuel property models built into SAS4A/SASSYS-1 for the fuel thermal conductivity, specific heat, and density. For the transient analysis, a fuel melting temperature of 1071°C, which is provided in Reference (Leibowitz, 1988), was assumed for FASTER's U-Pu-6Zr fuel.

For the cladding integrity limit, the peak cladding temperature can be used to estimate cladding wastage due to fuel-cladding eutectic formation. Cladding degradation due to eutectic penetration is a threshold reaction. The threshold for the FASTER's U-Pu-6Zr fuel was not available; however, for U-Zr fuel the eutectic formation has a threshold of 715°C. At temperatures near 715°C, the reaction is slow and it may take several hours for the cladding to fail. At higher temperatures, around 1075°C, fuel-cladding eutectic penetration occurs much more rapidly. However, for the transients that were analyzed, cladding temperatures exceed the long-term 715°C threshold for less than 30 seconds. Therefore, only a negligible amount of eutectic penetration will occur.

Of all the structures, the integrity of the reactor vessel is of the most concern since it provides the boundary for the primary circuit coolant. A limit of 732°C was used in the SAFR Preliminary Safety Information Document for the reactor vessel temperature and also applied to the redan structure. (DOE, 1985) In the absence of a detailed structural analysis for the preliminary FASTER design, this value was assumed for the structure and pool temperature limit.

3.2. UTOP

The unprotected transient overpower accident is initiated by an unintended withdrawal of the most reactive control rod over 15 seconds until it reaches a rod stop, which limits the reactivity insertion to 50¢. For the most reactive control rod, the rod stop would have to limit the control rod withdrawal to 8.6 cm to achieve 50¢. A 50¢ rod stop limit is larger than is typically assumed for SFR analyses. The 50¢ limit was initially selected because the worth per unit length of the control rods early in the FASTER design process was larger than for more traditional SFR designs. The control rod worth per unit length was decreased later in the design process but the 50¢ rod stop limit was maintained as a conservative assumption. For this UTOP analysis, the feedback coefficients due to control rod driveline and reactor vessel expansion were reduced to account for the control rod that has withdrawn and, therefore, does not contribute to those feedback effects.

3.2.1. UTOP at Beginning of Equilibrium Cycle

At the start of the BOEC UTOP transient, fission power increases due to the ramp reactivity insertion. After 15 seconds, a total of 50¢ has been inserted and the external reactivity insertion stops. As power increases, temperatures in the core increase quickly, introducing negative feedbacks that act to reduce the reactivity. When the external reactivity insertion stops at 15 seconds, total power has peaked at 155% and the net reactivity is at 12¢. Net reactivity then begins to decrease as the reactivity feedbacks become more negative.

Figure 5 illustrates the reactivity feedbacks during this transient. Fuel and cladding temperatures increase the fastest, producing -9¢ of reactivity from Doppler and -8¢ from axial core expansion. As sodium temperatures increase, the coolant density reactivity feedback introduces another -3¢ within the first minute. Twenty-five seconds into the transient, elevated structure temperatures at the above core load pads cause the core to expand radially, which inserts another -21¢ of reactivity. After 30 seconds, sodium temperatures in the upper internal structure increase and the drivelines begin to expand. The drivelines continue to expand, producing a reactivity feedback of -27¢. Within the first 60 seconds of the transient, net reactivity becomes negative and total power starts to decrease back towards 100%. Figure 6 illustrates power production during the BOEC UTOP scenario.

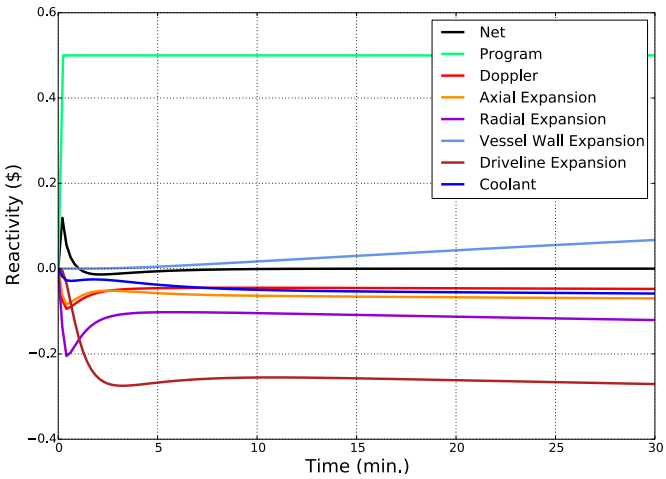

Figure 5: BOEC UTOP Reactivity Feedbacks

After 5 minutes, the hot pool temperature is leveling off while the cold pool temperature is still increasing. The reactor vessel expands as the cold pool heats up, which pulls the bottom-supported core away from the control rods and produces a positive reactivity feedback. The temperature rise in the hot pool is

a few degrees larger than the cold pool temperature rise so the control rod driveline expansion feedback produces more negative reactivity than the positive reactivity feedback from vessel expansion. The remainder of the transient is uneventful as net reactivity remains at zero and total power returns to slightly higher than 100%.

Fuel, cladding, and coolant temperatures, which are illustrated in Figure 7, were highest in Channel 8. The peak fuel temperature was 889°C, 23 seconds into the transient, and the minimum fuel melting margin decreased from 359°C to 182°C. At the same time, cladding temperatures peaked at 688°C, remaining below the 715°C threshold for slow eutectic formation. Coolant temperatures also peaked 23 seconds into the transient, reaching a maximum temperature of 657°C. The minimum margin to boiling was 292°C during the UTOP, occurring near the top of the assembly where the saturation temperature was lower due to the lower pressure.

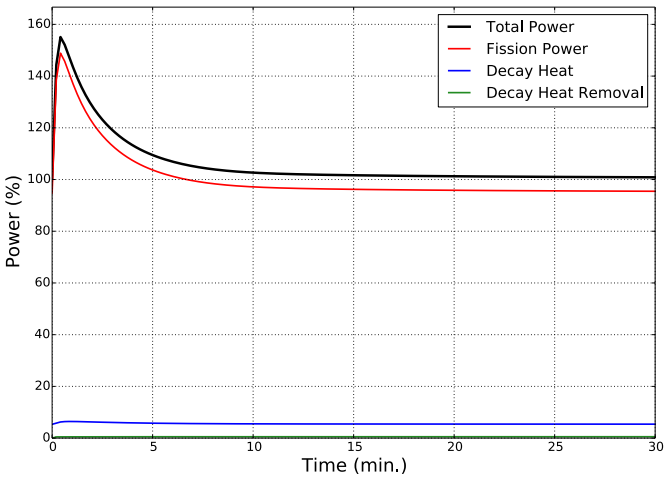

Figure 6: BOEC UTOP Total, Fission, and Decay Heat Power Production

The UTOP scenario progresses very quickly with temperatures peaking during the first half-minute and power decreasing back towards 100% after five minutes. For the rest of the transient, the peak temperatures in the core remain approximately 60°C higher than the initial steady-state temperatures. Because the core is producing slightly more than 100% of the steady-state power level and the steam generators are rejecting most of that, the DRACS heat rejection rate does not significantly affect the results. The transient progression with a total of 1.0% DRACS heat rejection instead of 0.5% produced nearly identical results.

3.2.2. *UTOP at End of Equilibrium Cycle*

The control rods are withdrawn at end of equilibrium cycle conditions so the transient initiator for this case does not apply.

3.3. *ULOHS*

The unprotected loss of heat sink accident is initiated by the intermediate sodium and feedwater pumps tripping. Because the steam generators are a boundary of the SAS4A/SASSYS-1 model, the resulting loss of heat rejection through the steam

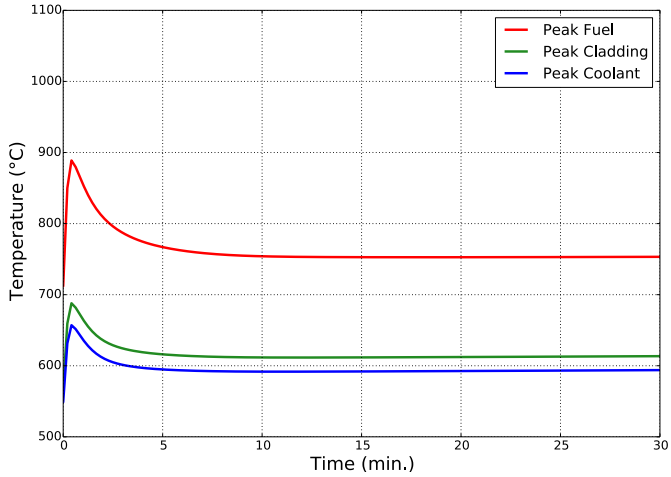

Figure 7: BOEC UTOP Peak In-Core Temperatures

generators was modeled by quickly reducing the temperature drop across the steam generators to zero at the start of the transient. This assumption is conservative as there would still be a small amount of heat rejection even after the feedwater pumps trip.

3.3.1. *ULOHS at Beginning of Equilibrium Cycle*

After the intermediate pumps trip, heat rejection through the intermediate heat exchangers decreases rapidly. The IHX primary-side outlet temperature begins to increase, causing the cold pool to heat up. The cold pool sodium mass is very large so the cold pool temperature increases slowly. The core inlet temperature increases at the same rate, introducing small but prompt negative feedbacks. Figure 8 illustrates the reactivity feedbacks during this transient. The axial core expansion and sodium density feedbacks are the strongest effects during the first two minutes, reaching -6¢ and -5¢, respectively. Together, these two feedbacks provide sufficient negative reactivity to drive the fission power down. At the same time, the reactor vessel begins to heat up and expand, which slowly pulls the core away from the control rods. Because the reactor vessel mass is so large, its temperature lags behind the increasing cold pool temperature so the reactor vessel expansion feedback is introduced slower than the in-core feedbacks. Before the reactor vessel expansion feedback exceeds 5¢, the net reactivity is less than -13¢ for more than four minutes.

Even as the core inlet temperature increases, the temperature rise across the core is decreasing, and the control rod drivelines become exposed to colder sodium discharged from the core. This introduces a positive reactivity feedback as the drivelines contract, partially withdrawing the control rods from the core. The control rod driveline temperature increases and decreases out of phase with the core inlet temperature, which introduces a power oscillation during the beginning of the transient, as shown in Figure 9. Fifteen minutes into the transient, when fission power is around 1%, the net reactivity becomes positive, and fission power increases to 3.6%. The core outlet temperature begins to increase again, causing the drivelines to heat up, which pushes the control rods back into the core. Net reactivity

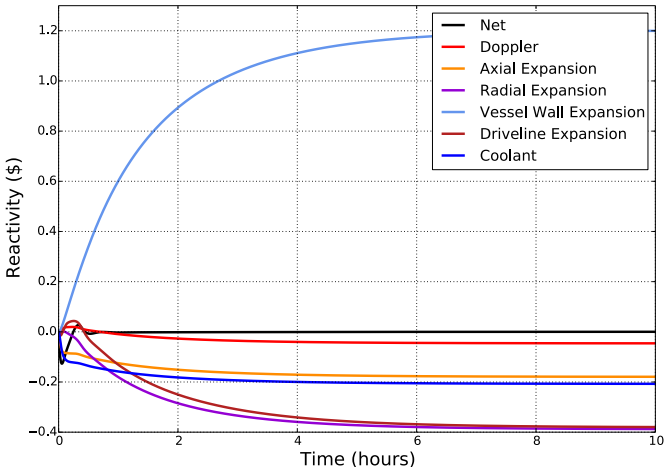

Figure 8: BOEC ULOHS Reactivity Feedbacks

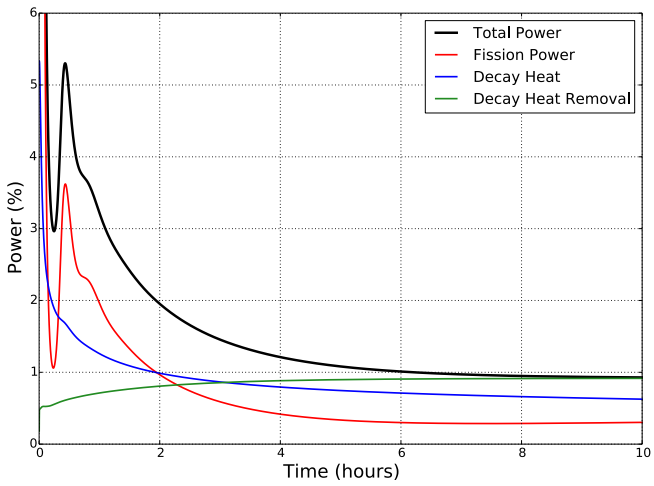

Figure 9: BOEC ULOHS Total, Fission, and Decay Heat Power Production

returns to zero 40 minutes into the transient after the control rod driveline and core inlet temperatures come into phase with one another.

Figure 10 illustrates temperatures in the primary system. During the rest of the first hour, primary system temperatures converge as total power decreases. Temperatures gradually increase until they are high enough for the DRACS heat rejection rate to match the total power level. The cold pool experiences the largest temperature increase, so the largest reactivity feedback effect is due to reactor vessel expansion. The radial core expansion and control rod driveline expansion feedbacks, and to a lesser degree the axial core expansion and sodium density feedbacks, are sufficiently large to balance out the very positive vessel expansion feedback and maintain a net reactivity of zero. Within 10 hours, the cold pool is hot enough that the DRACS heat rejection rate matches the total power production. As the transient continues, and decay heat continues to decrease, fission power increases to compensate for the decreasing decay heat to allow the system to remain in equilibrium at a power level of 0.9%.

Because net reactivity remains negative for the first 13 minutes of the transient and the primary pumps are still running, the peak fuel temperature never increases during the BOEC ULOHS. Peak cladding and coolant temperatures only rise 1°C and 15°C, respectively. There is no significant decrease in the fuel melting or sodium boiling margins. Clad temperatures do not increase enough for eutectic formation to be a concern and the maximum cold pool temperature is 562°C, well below the 732°C limit.

Analysis of the ULOHS transient at BOEC conditions was repeated with a nominal 1.0% DRACS heat rejection rate to confirm that 0.5% is sufficient. Results with the increased heat rejection were not significantly different. The DRACS heat rejection rate reached the total power production around 6 hours instead of 10 hours, and the system equilibrated at approximately 560°C instead of 562°C. Temperatures in the core decreased at the same rate at the beginning of the transient so the peak temperatures were nearly identical with the higher rejection rate. These results demonstrated that a 0.5% total DRACS heat rejection rate is sufficient and there is limited benefit of increasing to 1.0%.

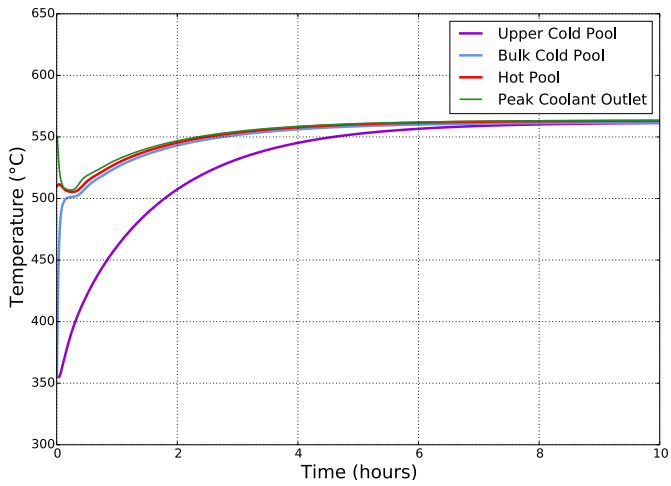

Figure 10: BOEC ULOHS Primary System Temperatures

3.3.2. *ULOHS at End of Equilibrium Cycle*

Because the control rods are withdrawn at EOEC, the EOEC ULOHS transient is much more benign than at BOEC conditions. Vessel expansion drives the ULOHS during BOEC conditions. But with the control rods already withdrawn at EOEC, the magnitudes of the vessel expansion and control rod driveline expansion feedbacks are significantly reduced. Temperatures throughout the primary system still converge around the steady-state hot pool temperature, but instead of having to oppose a large positive vessel expansion reactivity insertion, the negative feedback effects, particularly the coolant density and axial expansion feedbacks, drive net reactivity as low as -13¢ very quickly. Net reactivity remains negative until after the DRACS heat rejection rate exceeds the total core power production.

With the net reactivity remaining negative for several hours, instead of returning to zero as it does during the BOEC simulation, fission power drops to zero within 20 minutes, leaving

only the heat generated by decay heat. The DRACS heat rejection rate is sufficiently large that decay heat decreases below the heat rejection rate in less than 4 hours, and temperatures throughout the system begin to decrease.

In-core temperatures barely increase at the beginning of the transient. A boiling margin of 396°C is maintained. As with the BOEC cases, there is no significant decrease in the fuel melting margin and primary system pool temperatures remain well below the 732°C limit with the cold pool temperature peaking at 500°C, as illustrated in Figure 11. Cladding temperatures have also not increased enough for any eutectic formation. Peak in-core temperatures are illustrated in Figure 12.

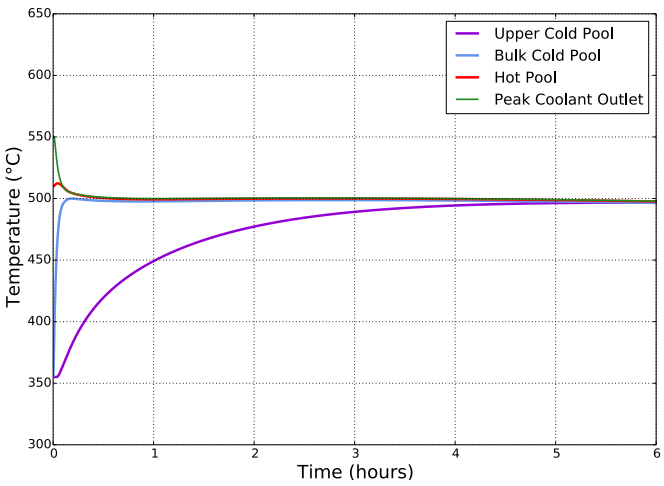

Figure 11: EOEC ULOHS Primary System Temperatures

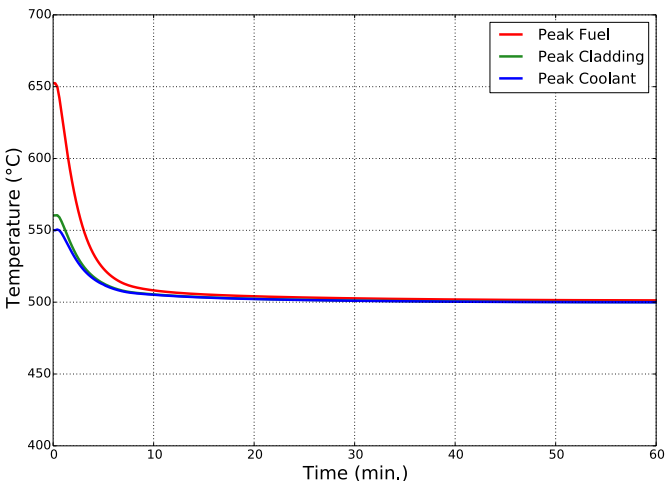

Figure 12: EOEC ULOHS Peak In-Core Temperatures

3.4. USBO

The unprotected station blackout transient is initiated by the primary, intermediate, and feedwater pumps simultaneously tripping. As the primary sodium pump design has not been completed, the USBO was simulated with a primary flow halving time of 10 seconds. As with the ULOHS transient, the loss of heat rejection through the steam generators was modeled by reducing the temperature drop across the steam generators to zero at the start of the transient.

3.4.1. USBO at Beginning of Equilibrium Cycle

The beginning of this transient is driven by an increasing power-to-flow ratio as the primary sodium flow rate decreases. Figure 13 illustrates the reactivity feedbacks during the beginning of the transient. Elevated core temperatures induce axial fuel and cladding expansion, producing a reactivity feedback of -8¢. Radial core expansion, which is driven by elevated structure temperatures at the above core load pads, reaches -31¢. As the fission power decreases, temperatures in the core begin to decrease and the net reactivity starts to become less negative. While the core is cooling down, hot sodium has been washing over the control rod drivelines, causing them to expand and push the control rods further into the core. Five minutes into the transient, the CRDL feedback reaches -54¢.

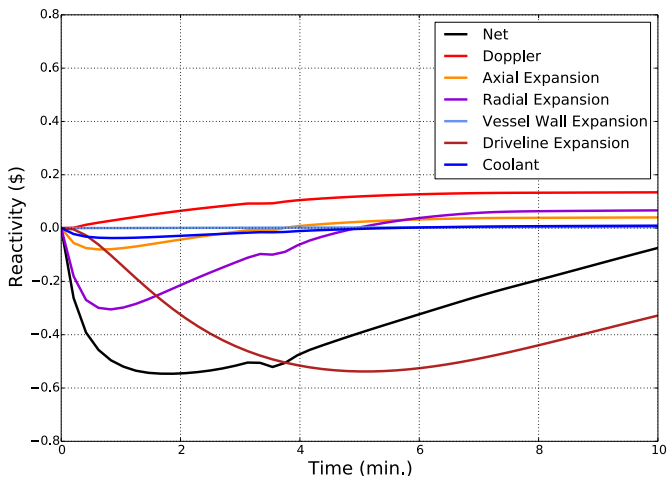

Figure 13: BOEC USBO Reactivity Feedbacks

As power decreases, the core outlet temperature begins to decrease. The control rod driveline temperature decreases and the CRDL feedback becomes less negative. Out-of-phase temperature changes in the core and for the drivelines cause the net reactivity to become positive at 11 minutes. Doppler, radial core expansion, axial expansion, and the coolant density feedbacks become temporarily positive. Net reactivity peaks at 10¢ before the hotter temperatures in the core induce another negative response from the in-core reactivity feedbacks, particularly radial expansion. The 8-minute period of positive net reactivity causes fission power to increase from close to zero to 3 MW before the net reactivity becomes negative again and the fission power begins to decrease.

Because the feedwater pumps have tripped, the only heat rejection is through the DRACS units. For the remainder of the transient, net reactivity remains at or slightly below zero. Fission power decreases gradually but a low enough system temperature is maintained that fission power remains around 0.2% power for most of the transient. Decay heat also keeps decreasing until total power matches the heat rejection capacity of the decay heat removal system around 17 hours. The amount of

time before heat rejection matches total power production is longer than for the ULOHS transient because lower cold pool temperatures are maintained during the USBO transient, and so the DRACS heat rejection rate is lower. More time is required for the cold pool temperatures to gradually increase and decay heat production to decay away.

The highest in-core temperatures occur during the first minute of the transient. The peak fuel temperature only increases from 712°C to 741°C, so a very large fuel melting margin is maintained. Cladding temperatures increase close to the fuel temperatures, reaching a peak of 720°C. This is slightly above the threshold for slow eutectic formation; however, cladding temperatures remain above the threshold for less than 30 seconds so there is no significant cladding reduction due to fuel-cladding eutectic penetration. Sodium temperatures in the core peak at 719°C and a sodium boiling margin of 234°C is maintained. With a maximum cold pool temperature of 462°C, long-term structural stability is not a concern for the reactor vessel. Figure 14 illustrates the peak in-core temperatures at the beginning of the transient.

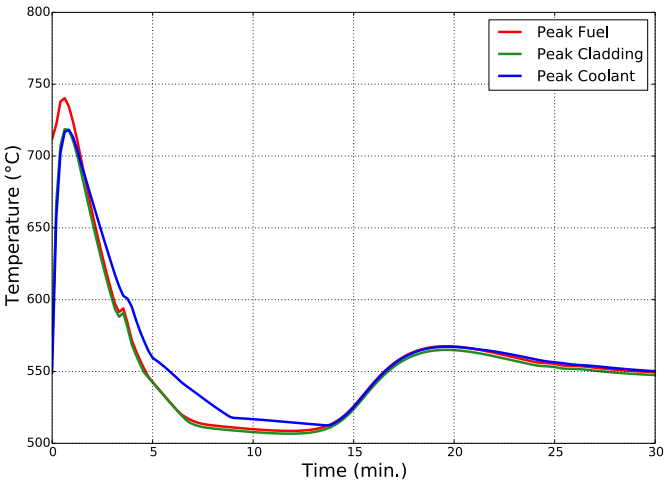

Figure 14: BOEC USBO Peak In-Core Temperatures

The BOEC USBO transient was simulated a second time with a nominal heat DRACS heat rejection rate of 1.0%. With a heat rejection rate 0.5%, fission power remained at approximately 0.2% in order to maintain equilibrium between heat rejection and total power. With 1.0% DRACS heat rejection, decay heat decreases at a similar rate so more fission power is necessary to maintain the power balance. Even with the higher fission power level at the end of the transient, the peak fuel, cladding, and coolant temperatures are unchanged because they are still occurring during the first minute of the transient, before the heat rejection rate affects temperatures in the core. This confirmed that the smaller 0.5% heat rejection rate was sufficient because it produced the same safety margins as the 1.0% heat rejection rate while maintaining a lower power level for the duration of the simulation.

3.4.2. USBO at End of Equilibrium Cycle

The USBO was also simulated at EOEC. During the first few minutes of the transient, before the control rod driveline and reactor vessel expansion feedbacks influence the results, the reactivity feedbacks are very similar to the BOEC results. The cold pool temperature increases more than the hot pool temperature so reactor vessel expansion is larger than the control rod driveline expansion. However, because the control rods are already withdrawn, the reactivity feedback due to the change in the control rod insertion depth is very small. Net reactivity decreases to -48¢ within the first few minutes, and because the driveline expansion feedback is smaller than for the BOEC case, the out-of-phase driveline and core inlet temperatures only produce small fission power swings. Where net reactivity rebounded to 10¢ for the BOEC case, net reactivity rebounds only to 1.5¢ at EOEC. The long-term behavior of the EOEC case is similar to the BOEC case. The biggest difference is that while power remained at approximately 0.2% for the BOEC case, fission power is essentially zero within 4 hours for the EOEC case. Decay heat slowly decreases until total power drops below the DRACS heat rejection capacity at 8 hours. As with the BOEC case, the peak temperatures occur within the first minute. The safety margins are all larger at EOEC with fuel, cladding, and coolant temperatures all remaining below 700°C for the EOEC USBO. Figure 15 illustrates the reactivity feedbacks during this transient and Figure 16 illustrates power production and decay heat rejection.

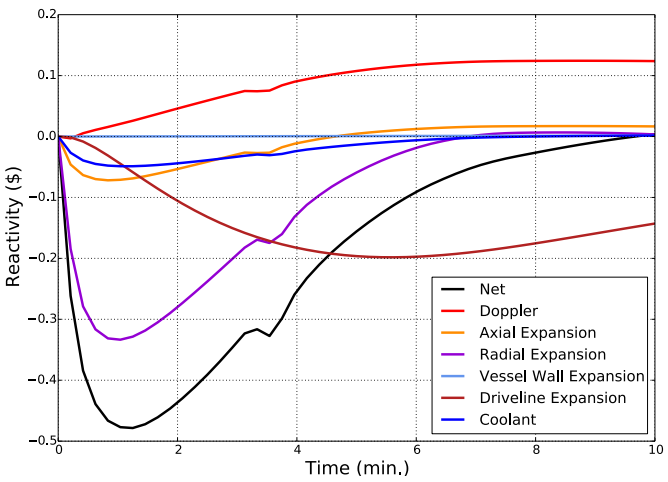

Figure 15: EOEC USBO Reactivity Feedbacks

4. Summary and Conclusions

Three types of beyond design basis transient scenarios were analyzed for the FASTER design: unprotected transient overpower, unprotected loss of heat sink, and unprotected station blackout. These transients were simulated using SAS4A/SASSYS-1 at both beginning of equilibrium cycle and end of equilibrium cycle conditions, except for the UTOP scenario, which was only simulated at BOEC conditions. For each transient, failures of both the primary and secondary reactor scram systems were assumed.

The selection of liquid sodium coolant and metallic fuel with a pool-type primary system arrangement provides a highly reliable reactor system with large safety margins between normal

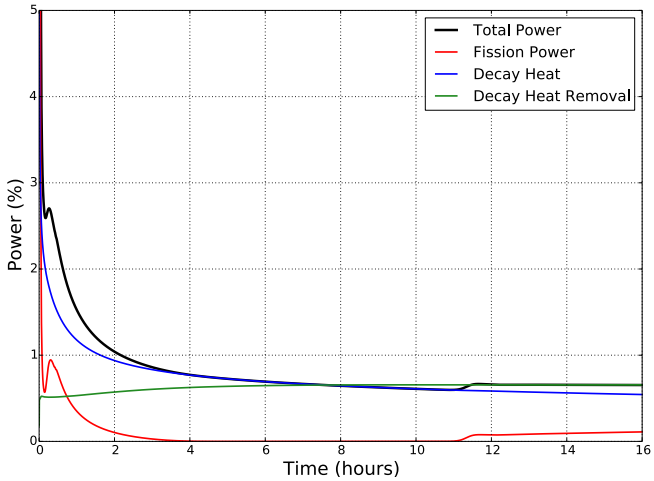

Figure 16: EOEC USBO Total, Fission, and Decay Heat Power Production

operating conditions and limiting failure conditions. Sodium provides effective heat removal and transport characteristics at low operating pressure with a large temperature margin to boiling. Although the metallic U-Pu-6Zr fuel has a low melting temperature, its high thermal conductivity means that it operates at temperatures below the coolant boiling point. And the choice of a pool-type primary system provides a large heat sink during transient conditions as well as a shutdown heat removal path via natural circulation.

Additionally, the favorable reactivity feedbacks lead to relatively low peak fuel, cladding, and coolant temperatures during the analyzed transients and the reactor vessel temperature remained well below the limit for ensuring structural stability. Tables 6 and 7 list the predicted peak temperatures and safety margins, respectively, for the BOEC transients and EOEC transients. With such large safety margins maintained during these highly events, these results demonstrate FASTER's inherent passive safety capability.

Table 6: Peak Temperatures for BOEC and EOEC Transients

Beginning of Equilibrium Cycle Conditions				
	Coolant	Cladding	Fuel	Reactor Vessel
Nominal	549(°C)	568(°C)	712(°C)	355(°C)
UTOP	657(°C)	688(°C)	889(°C)	415(°C)
ULOHS	564(°C)	569(°C)	712(°C)	562(°C)
USBO	719(°C)	720(°C)	741(°C)	462(°C)

EOEC Conditions				
	Coolant	Cladding	Fuel	Reactor Vessel
Nominal	550(°C)	560(°C)	652(°C)	355(°C)
ULOHS	551(°C)	561(°C)	653(°C)	500(°C)
USBO	684(°C)	684(°C)	694(°C)	431(°C)

Table 7: Safety Margins for BOEC and EOEC Transients

Beginning of Equilibrium Cycle Conditions				
	Sodium Boiling	Rapid Clad Eutectic	Fuel Melting	Reactor Vessel Failure
Nominal	398(°C)	507(°C)	359(°C)	377(°C)
UTOP	292(°C)	387(°C)	182(°C)	317(°C)
ULOHS	391(°C)	507(°C)	359(°C)	170(°C)
USBO	234(°C)	355(°C)	330(°C)	270(°C)

EOEC Conditions				
	Sodium Boiling	Rapid Clad Eutectic	Fuel Melting	Reactor Vessel Failure
Nominal	398(°C)	515(°C)	419(°C)	377(°C)
ULOHS	396(°C)	514(°C)	418(°C)	232(°C)
USBO	268(°C)	391(°C)	377(°C)	301(°C)

5. Acknowledgment

This work is supported by the U.S. Department of Energy, Office of Nuclear Energy, under contract #DE-AC02-06CH11357.

References

D. Petti (INL), R. Hill (ANL), J. Gehin (ORNL)., 2016. Advanced Demonstration and Test Reactor Options Study. INL/EXT-16-37867, Idaho National Laboratory, Argonne National Laboratory, and Oak Ridge National Laboratory.

DOE, 1985. SAFR - Sodium Advanced Fast Reactor. Technical Report. Preliminary Safety Information Document, AI-DOE-13527, Initial Issue.

F. Heidet, e.a., 2018a. Fast Test Reactor (FASTER) Design Overview. Manuscript submitted for consideration to Progress in Nuclear Energy .

F. Heidet, e.a., 2018b. FASTER Core Design. Manuscript submitted for consideration to Progress in Nuclear Energy .

Fanning, T. H., ed., 2017. The SAS4A/SASSYS-1 Safety Analysis Code System. Technical Report. ANL/NE-16/19, Nuclear Engineering Division, Argonne National Laboratory.

INTERNATIONAL ATOMIC ENERGY AGENCY, 2017. Benchmark Analysis of EBR-II Shutdown Heat Removal Tests, IAEA-TECDOC-1819. Technical Report. IAEA, Vienna.

K. L. Basehore and N. E. Todreas, 1980. SUPERENERGY-2: A Multiassembly, Steady-State Computer Code for LMFBR Core Thermal-Hydraulic Analysis. Technical Report. Pacific Northwest Laboratory, PNL-3379, COO-2245-57TR.

Leibowitz, L., E. Veleckis, and R. A. Blomquist., 1988. Solidus and Liquidus Temperatures in the Uranium-Plutonium-Zirconium System. Journal of Nuclear Materials 154, 145–153.

Smith, M. A., C. Adams, W. S. Yang, and E. E. Lewis., 2013. VARI3D & PERSENT: Perturbation and Sensitivity Analysis. Technical Report. Argonne National Laboratory, ANL/NE-13/8.

Smith, M. A., E. E. Lewis, and E. R. Shemon., 2014. DIF3D-VARIANT 11.0, A Decade of Updates. Technical Report. Argonne National Laboratory, ANL/NE-14/1.